AD-755 243

SONAR MAPPING OF THE UNDERSIDE OF SEA ICE

C. S. Clay, et al

Wisconsin University

Prepared for:

Office of Naval Research
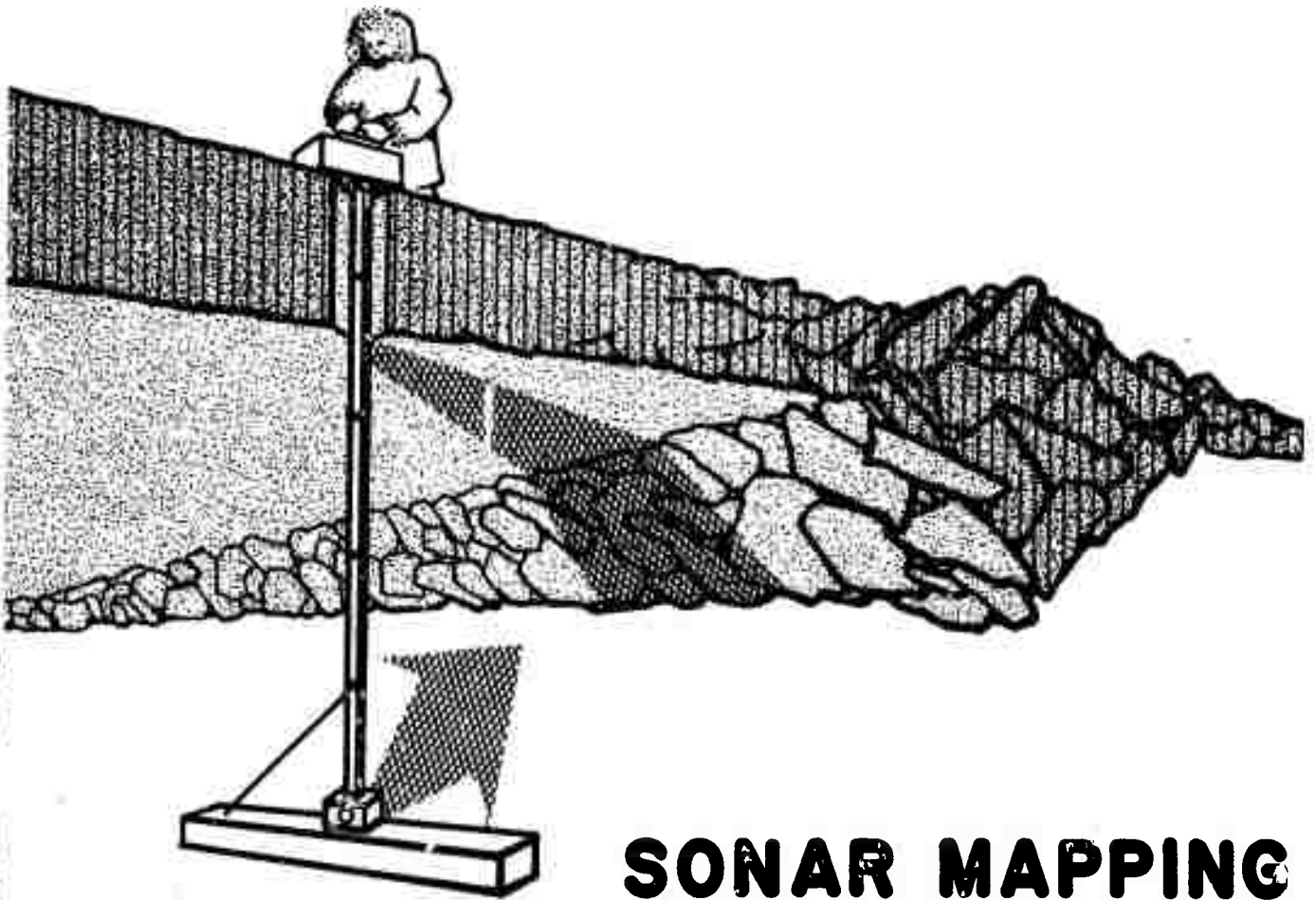Advanced Research Projects Agency

February 1972

AD755243

SONAR MAPPING
OF THE UNDERSIDE OF SEA ICE

FINAL REPORT

C S   CLAY

J M   BERKSON

T K   KAN

RESEARCH   REPORT
No 73-1   FEB 1973

21-

SONAR MAPPING OF THE UNDERSIDE OF

SEA ICE

BY

C. S. Clay, J. M. Berkson and T. K. Kan

The University of Wisconsin
Department of Geology and Geophysics
Geophysical and Polar Research Center
6118 University Avenue
Middleton, Wisconsin 53562

Contribution No. 293

Final Technical Report

ARPA Order Number
    1783/3-31-71

Program Code Number
    415 ONR

Name of Contractor
    University of Wisconsin

Effective date of Contract
    June 15, 1971

Contract Expiration Date
    June 14, 1972

Amount of Contract
    $50,414

Contract Number
    N00014-67-A-0128-0019

Principal Investigator and Phone Number
    C. S. Clay
    (608) 262-1921

Scientific Officer
    Director, Arctic Program
    Earth Sciences Division
    Office of Naval Research
    Dept. of the Navy
    800 N. Quincy St.
    Arlington, Va. 22217

Short Title of Work
    Arctic Basin Technology: Sonar
    Measurements of the Bottom of
    Ice in the Arctic

ABSTRACT

A technique was developed for adapting the side-scan sonar to obtain sonar maps of the undersurface of sea ice. The equipment is portable and air-mobile operations were made from single-engine light aircraft. Graphic records displaying the range and relative scattering strengths at 48 kHz were assembled into sonar maps that display the location and shape of underice features. Data were taken at five sites in the Arctic: (1) 2 km from Pt. Barrow, Alaska, (2) a hydrohut near Fletcher's Ice Island (T-3), (3) 2 km from the edge of T-3, (4) 175 km from Pt. Barrow, Alaska, (5) the AIDJEX main camp. The data indicate that for pack ice there are two distinct types of backscattering: very high level backscattering from well defined underice ridges and very low level backscattering from between the ridges. The higher scattering at the ridges is probably due to the increase in roughness and the tilting of the average plane of the scattering surface. Comparison of the sonar map and the aerial photograph shows that most surface features have subsurface expressions and their relationships can be complex.

PURPOSE

The purpose of the research is:

To develop the underwater technology required to measure the location and shape of features on the bottom of sea ice and to compare the bottom with features on the surface; and to study the scattering of sound from the water-ice interface.

INTRODUCTION

Bottom-scanning sonar has been used to measure the geographical location of features on the sea floor since World War II.[1] The morphology

and sound scattering are related as follows: large rocks, gravel beds, etc., scatter signals; over smooth bottoms, relatively little energy is scattered back.[2] Somewhat independently, sonar bottom reverberation measurements have shown quantitative differences in the scattering over different kinds of bottom.[3] Sonar reverberation measurements have been made over bottoms described as mud, sand, and rocks and the scattering strength of mud is usually much lower than sand and rock. The two approaches need to be put together. Theoretical studies of the high frequency round scattered at rough surfaces have shown the back scattered to be dependent upon the material of the bottom, its shape, and to a lesser extent the frequency of the signal (for roughness much greater than the acoustic wave length).[4]

Side-scanning sonar records of the bottom of sea ice may yield information about the morphology of sea ice and scattering of sound from the sea-ice bottom.

METHOD

Figure 1 shows the sonar geometry beneath the ice. The sonar transducer is on a rotating mount so that it can be lowered through a 23 cm hole that is drilled with a gasoline-driven ice auger. The support assembly consists of 1.9 m aluminum sections that can be rotated at the surface. The transducer can be lowered to any depth and its direction can be controlled to less than 1°. The sonar is a modified Kelvin Hughes Transit Sonar that transmits a 1 msec ping at 48 kHz. The beam is fan shaped with a beamwidth of 1½° in the horizontal and 51° in the vertical. Underice features, such as the ridge in Figure 3, scatter sound back to the transducer. The range and relative backscattering level are displayed on an
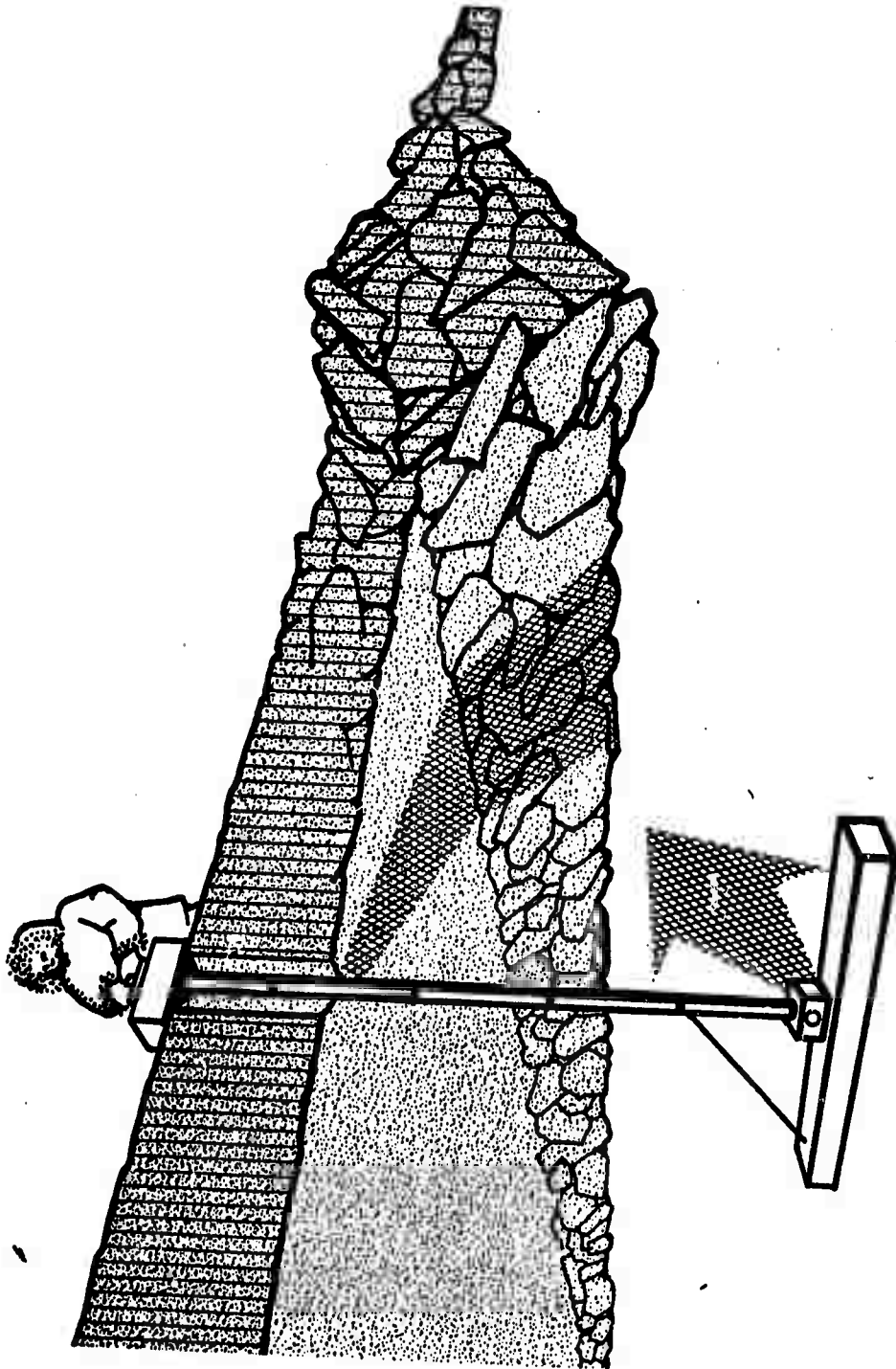
Figure 1. Underice Sonar.

intensity-modulated graphic recorder. The recorder has a dynamic range
of about 20 db from white to black. A time-variable gain is used to com-
pensate for the signal level decrease as range increases. Beyond 25 m,
we were able to adjust the time-variable gain so that the record was
marked at the same intensity for comparable scattering features out to
the maximum range. Once it is adjusted, normally the gain is the same at
the same range for subsequent transmissions. Maximum ranges of 275 m and
550 m are obtained with this system. A picture of the scattering character
of the ice bottom is made by rotating the transducer in increments. The
data are displayed by assembling display increments in a polar mosaic.

Underice sonar measurements were made at 5 sites, Figure 2. The first,
near Pt. Barrow, Alaska, was used for instrumentation tests. The others
were Fletcher's Ice Island (T-3), pack ice and the AIDJEX main camp.

An example of a sonar map, taken under pack ice about 175 km from
Pt. Barrow, Alaska is shown in Figure 3. The transducer was at depth 8.8 m
and the ice thickness was 1.5 m. For easier visualization of the data, we
assembled the sonar scattering mosaic using 3° sectors (Fig. 4). The data
were taken at different gain steps to increase the dynamic range of the
display and because we experienced changes in the overall receiver gain
during the experiment. Temperature- or velocity-depth profiles were not
made, but other measurements taken under arctic sea ice for this season
suggest a nearly iso-velocity sound structure for our working depths.[5,6]
Since the transducer depth below the underice surface is much less than
the scan ranges of the sonar, the slant ranges shown by the map are approx-
imately equal to the true ranges of the underice features. The sonar map
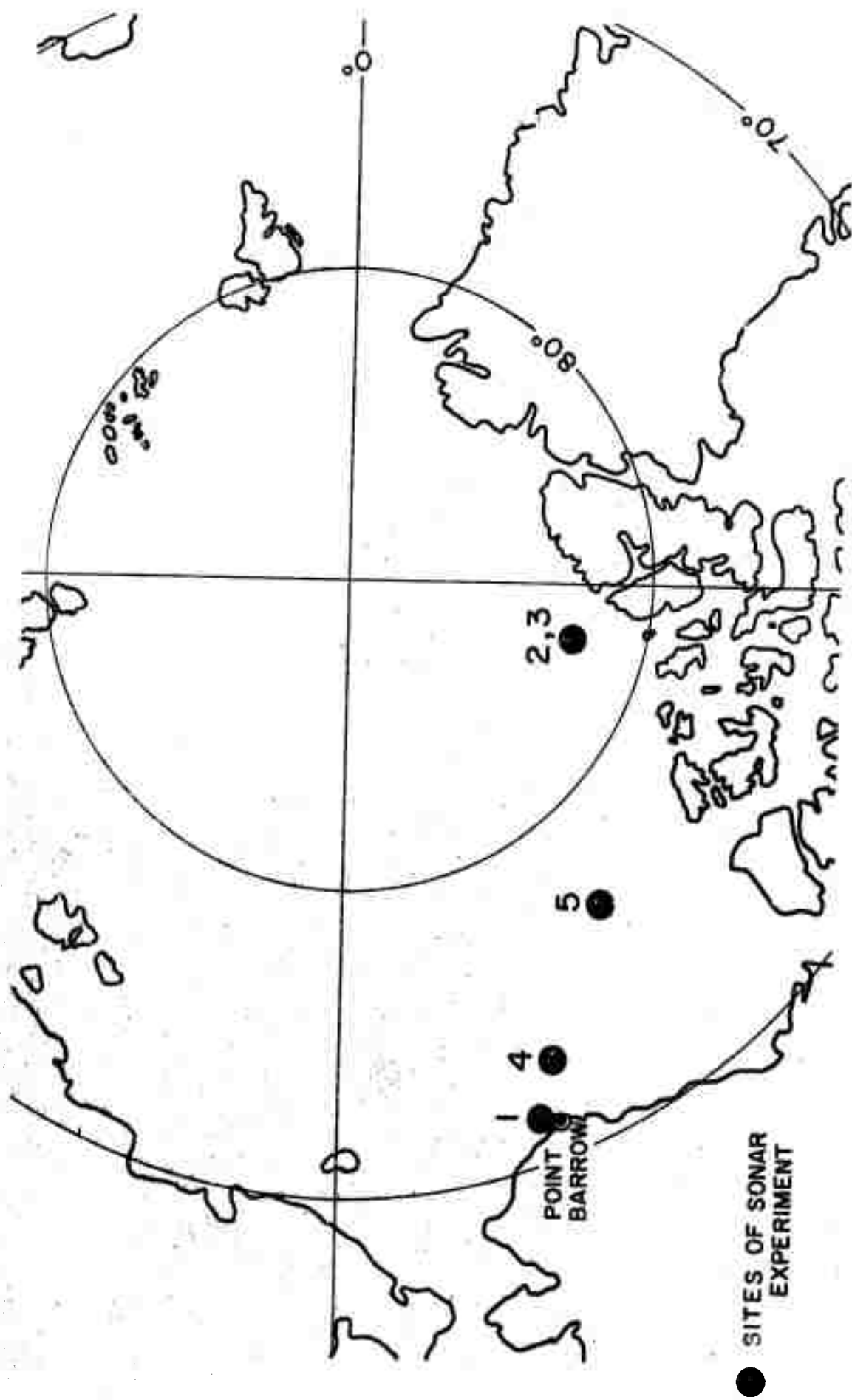then represents a plan view of underice features that scatter sound.

Figure 2. Areas of Investigation: #1: 2 km from Pt. Barrow, Alaska; #2: Hydrohut near Fletcher's Ice Island (T-3); #3: 2 km from the edge of T-3; #4: 175 km from Pt. Barrow; #5: AIDJEX main camp.
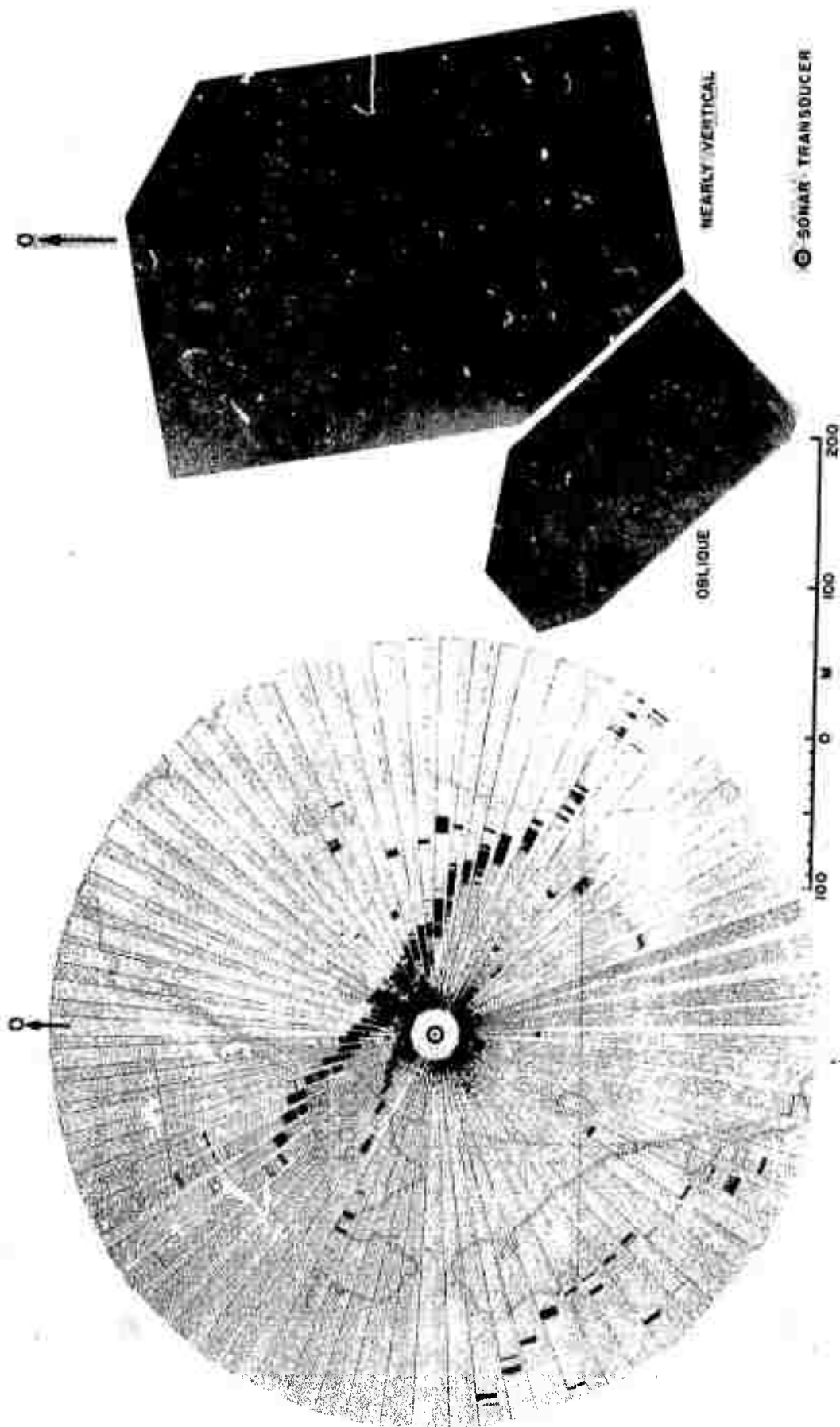
Figure 3. Comparison of Underice Sonar Map (left) and Aerial Photograph of the Sea Ice Surface (right). The data were taken at a site about 175 km north of Barrow, Alaska. The ice thickness at the sonar hole was 1.5 meters and the transducer was at 8.8 meters depth. The underice ridge at the top is generally deeper than the sonar transducer, and thus blocks sound from reaching most areas beyond it. Sonar maps taken at different transducer depths give additional information about the nature of the underice surface. The smoke grenades were used as reference points.

The sonar map shown in Figure 4 shows the edge of Ice Island T-3 and the sea ice of Colby Bay that remains attached to the ice island.

UNDERICE MORPHOLOGY

The relationship between surface features and underice features is studied by comparing the sonar maps and aerial photographs. Figure 3 shows that most of the surface features have subsurface expressions. An underice ridge will generally scatter sound only from the side facing the transducer and the other side will be in shadow. The data are superimposed on Figure 4. At this site, the width of the scattering side varies from about 1 to 3 times the width of the surface expression. The prominent subsurface ridge (55 m range at 0° and the ridge trend is 130° clockwise) is generally deeper than the transducer and has blocked sound from reaching most of the underice surface beyond it. The relationship between underice features and surface features can be complex. For example, in Figure 4, the underice expression of the farther surface feature appears to be approximately symmetrical with its surface ridge, whereas the underice expression of the near feature appears to be located only on one side of the surface ridge.

Sonar data were taken in from a hydrohut on T-3. A sonar map is shown on Figure 5. We did a number of experiments to test underice sonar techniques such as using a vertical transducer for depth contouring.[7] The interference patterns of a pair of transducers were used to make iso-angle contours of the underice surface,[8] but we did not obtain identifiable zebra stripes. In the smooth areas of the underice surface, the scattering levels were too low to observe the zebra stripes and in the rough areas, the ridges were too rough to follow the zebra stripes. We made measurements through
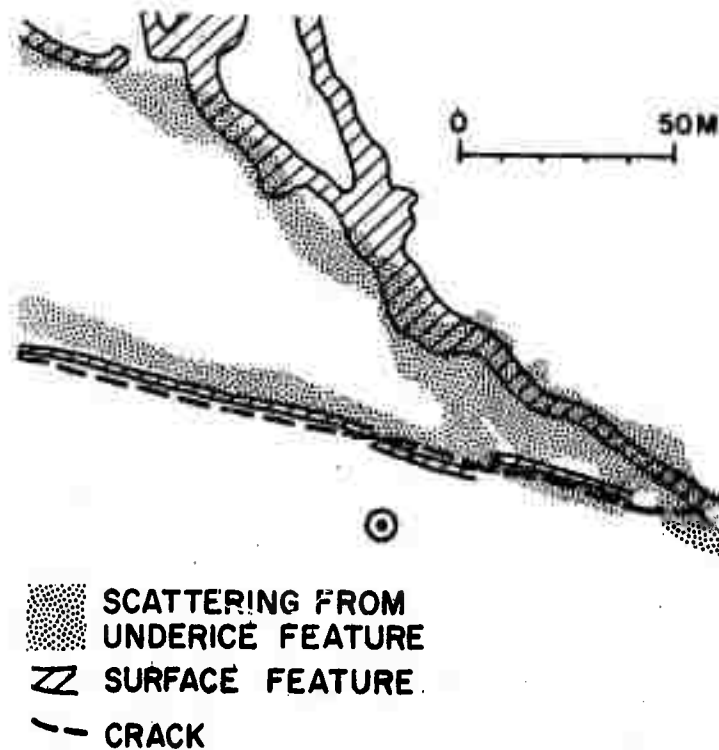
Figure 4. Relationship of Surface Features and Underice Scattering Based on the Sonar Map and Aerial Photograph. Surveyed control points indicate that the aerial photograph has negligible distortion in this area. An underice ridge will scatter sound only from the side facing the transducer, and the other side will be in shadow. The underice ridge at the top appears to be more or less symmetrical with its surface expression; whereas, the lower underice ridge appears to be a projection located only on one side of its surface expression.
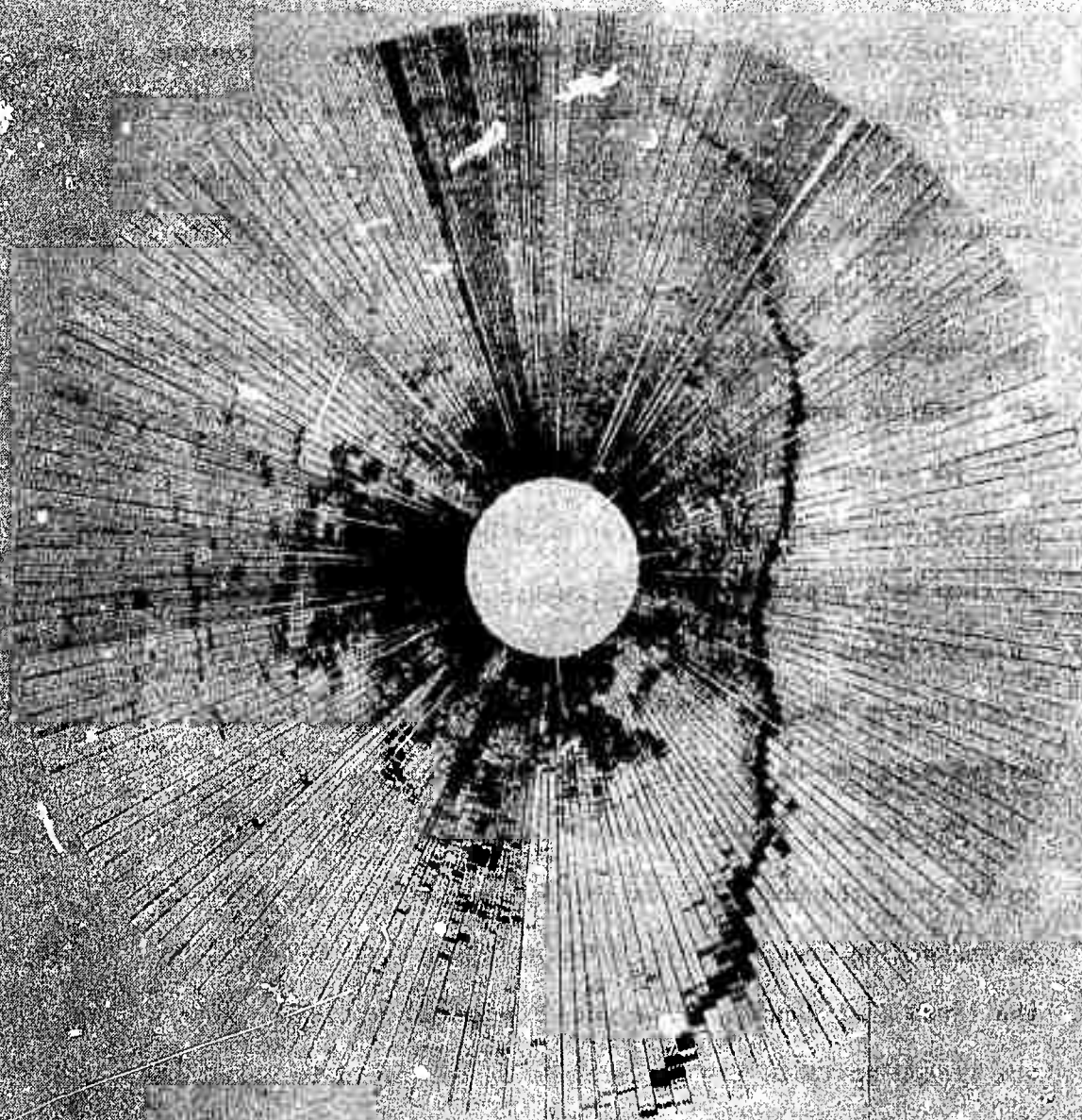
COLBY BAY, T-3 (84°22'N 84°31'W), 21 APR 72
LAMONT HYDROHUT, DEPTH 14.6M ICE 3.8M

Figure 5. Sonar map showing edge of ice island (T-3) and the sea ice of Colby Bay that remains attached to the ice island. The edge of T-3 is the strong reflection on the right side of the map.

the hole in a hydrohut near T-3 with a crossed pair of transducers to obtain a pencil beam.

Most of our depths were measured by placing the transducer in the vertical position. We found that this technique has problems with resolution because of the wide horizontal beam and the vertical side lobes. The results are useful but we learned that it will be desirable to shade the transducers to reduce the side lobes. Additional information was obtained by studying the changes of the reflections and shadows on sonar maps taken at different depths.

Both sonar and surface surveys were carried out at site #3. Seven sets of data were taken. Three sets have a narrow horizontal beam and four of them have a narrow vertical beam. On Figure 6, a surface map superimposed on a sonar map is shown. We have estimated the subsurface elevations of the features by using the information collected from those four sets of narrow-vertical-beam data.

The surface survey included a survey across a ridge. We have shown on Figure 7 the underice scattering features, the survey path and the corresponding cross-section. The estimated sail heights, keel depths and the ratio keel depth/sail heights for the four ridges shown on Figure 7 are listed in Table I. The average of the ratio is 7.1.

Table I

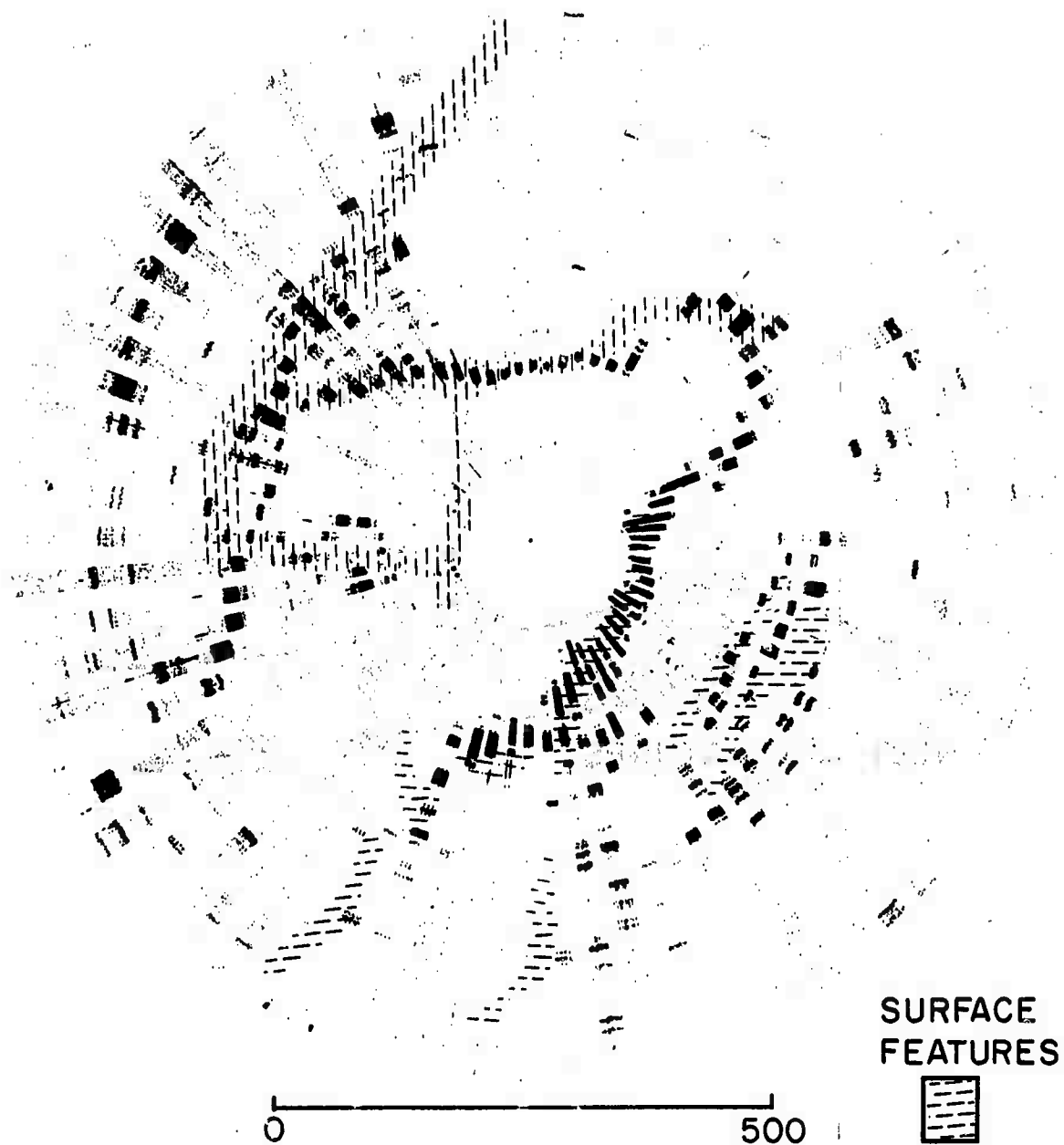| Estimated Peak Top Elevation	Estimated Keel Depth	Ratio	$\frac{Keel\ depth}{height}$
1.425 m	10 m		7
1.17 m	9 m		7.69
1.5 m	11 m		7.25
1.48 m	10 m		6.75

Figure 6. Sonar map and surface features on pack ice near Fletcher's Ice Island (T-3), April 1972.
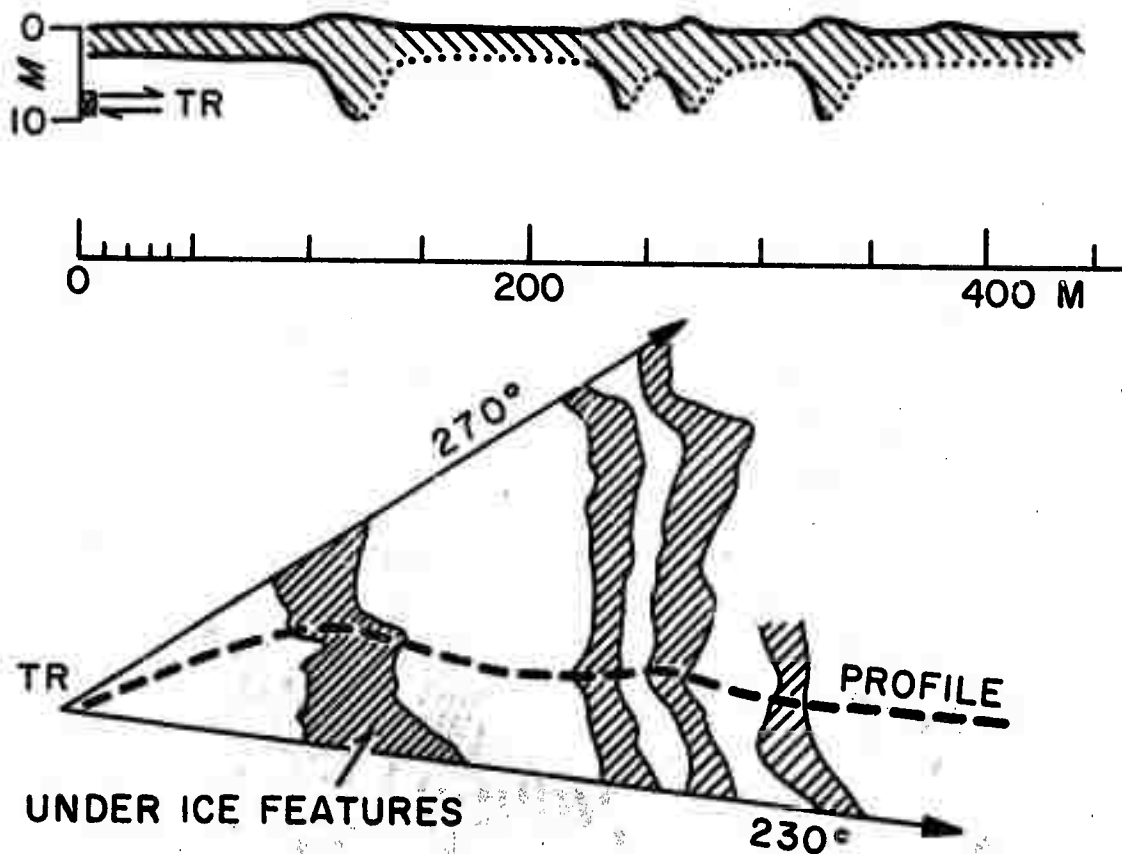
Figure 7. Scattering features and profile of pack ice. The surface elevations were measured along the survey path. Underice depths are from sonar data. The dotted portions are in shadowed regions for the sonar.

The University of Washington Applied Physics Laboratory's subsurface
vessel (UARS) surveyed the ice under Colby Bay area, and part of its four
tracks extended into our survey area. Their results agree well with ours
(Robert Francois, written communication, 1972).

The morphology of the undersurface of the sea ice of site #4, and the
relationship with the top surface are discussed by Berkson, Clay and Kan,
1973, Journal of the Acoustical Society of America, in press. Sites #2
and #3 were discussed by Berkson, Clay and Kan, 1972, American Geophysical
Union Fall Meeting. Sites #3 and #5 are discussed by Kan (M.S. thesis,
1973); Kan, Clay and Berkson (in preparation, 1973); and Clay, Kan and
Berkson (in preparation, 1973).

SCATTERING OF SOUND

The data show very low backscattering levels at 48 kHz of the under-
ice surface between the ridges and very high levels at the ridges. The
relatively flat underice areas between the transducer and the first ridge
will always be illuminated; but beyond the first underice ridge, areas may
be in shadow. The length of the shadow depends on the downward projection
and the transducer distance and depth. In Figure 3, the relatively flat
areas between the transducer and the first ridges are characterized by very
low backscattering. (The scattering near the transducer may be large but
the rapid change of the time-variable gain precludes qualitative estimates
of scattering for ranges less than 25 m.) The very low values are indi-
cated by the lack of any contrast between the backscattering background of
the underice surface between the ridges and the shadow zones behind promi-
nent underice ridges, even at the highest gain steps. However, there is
very high backscattering from well-defined areas of the underice surface

which generally have surface expressions. Qualitatively, the scattering cross sections at ridges are at least 20 db greater than the flat areas.

In the conventional backscattering experiment, the backscattering levels vs. time or angle are measured and the backscattering function (scattering cross section vs. angle of incidence or grazing angle) is derived from the geometry of the measurement and ray tracing. If an omnidirectional source and receiver are used, one usually assumes that the scattering interface has statistical spatial stationarity for data analysis.[5] For example, if the scattering is from features of the order of a few cm, then any area of the order of a few square meters should have the same roughness as any other area. Then, the observed backscattering function may be compared to theoretical functions for rough surfaces. Let us consider another model consisting of smooth surfaces surrounding rough patches at random distances. In omnidirectional backscattering experiments, the nature of the scattering surface would not be revealed because the addition of the backscattered signals coming from all directions could give relatively smooth backscattering functions such as those observed in measurements.[5,9,10,11] The amount of backscattering would increase with both the roughness of the patches and number of patches.

A number of authors have reported that backscattering levels from the undersurface of sea ice are anomalous, that is, not the scattering function expected from an isotropic uniformly rough surface. Mellen[12] noted that there are discrepancies between scattering theory and underice data. The theory does not predict the observed backscattering functions, and the underice spatial roughness spectrum deduced from backscattering functions is significantly higher than the spectrum derived from upward-looking,

narrow-beam sonar profiles taken by submarines. Greene[13] found at a pack-ice site that backscattering strengths increase as the angle of incidence increases. The scattering from sea ice is large, as much as 40 db greater than from the wind-blown, ice-free sea surface.[11] As expected, backscattering from the underice surface tends to increase with increasing surface roughness of a site.[14]

Our data show two distinct types of underice surfaces: the underice ridges and the relatively smooth areas between the ridges. The differences in scattering at these interfaces may be due to differences in slope of the interface, in reflection coefficient, or in roughness. Theory shows the following: (1) scattering cross sections generally decrease as the incident angle θ tends to 90°. The shape of the function is sensitive to the spectrum of the roughness. (2) The scattering is proportional to the reflection coefficient squared. (3) The cross section depends upon the rms roughness relative to the acoustic wavelength and the cross section is asymptotic to a limiting value for very short wavelengths.

We now apply the basic theory and a model of the underside of the ice (Fig. 8) to scattering measurements. At the smooth surface θ is larger than θ at the ridges. The reflection coefficient is probably smaller at the smaller angle of incidence (Langleben and Pounder[15] report that the reflection coefficient is 0.1 near 0° and increases rapidly for θ greater than 30°). Since our data show the scattering from the ridges to be large, the increase of roughness and decrease of θ compensates for any decrease in the reflection coefficient. As viewed from a transducer located below a smooth area (between ice ridges), the sound beam intercepts more ridges at smaller grazing angles and one would expect the average scattering to
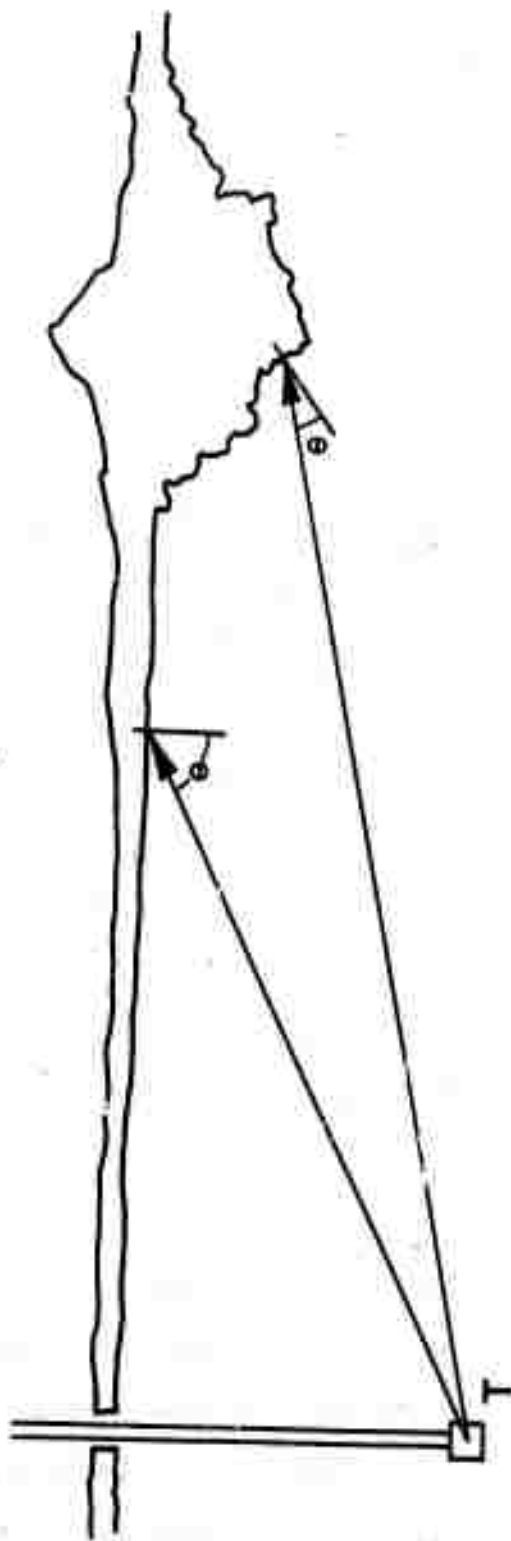
Figure 8. Sonar Geometry below sea ice.

increase at small grazing angles. This could account for the anomalous scattering function reported by Greene.[13]

In attempting the inverse problem of determining the properties of the rough ice undersurface from backscattering measurements we see obvious problems. Most of the scattering comes from localized patches associated with the undersides of ice ridges. The average plane of these scattering patches may be inclined 30° or more relative to the horizontal. This information would have to be included in calculating scattering coefficients as a function of grazing angle. If the area of the scattering patch is less than the resolution of the transducer, then this must also be included in the data reduction. An average reflection coefficient should be determined for the patch. The spatial spectrum associated with the scattering cross section is then that for the rough patch. Presumably the smooth areas would have their own scattering functions and spatial roughness. These difficulties could account for the lack of agreement between theory and data noted by Mellen.[12]

ACKNOWLEDGMENTS

References

1. Chesterman, W. D., P. R. Clynick, and A. H. Stride, An acoustic aid to sea bed survey, Acustia 8, 285-90, 1958.

2. Wong, H. K. and W. D. Chesterman, Bottom backscattering near grazing incidence in shallow water, J. Acoust. Soc. Amer. 44, 1713, 1968.

3. McKinney, C. M. and C. D. Anderson, Measurement of backscattering of sound from the ocean bottom, J. Acoust. Soc. Amer. 36, 158, 1964.

4. Tolstoy, I. and C. S. Clay, Ocean Acoustics, McGraw-Hill, New York, 1966.

5. Milne, A. R., Underwater backscattering strengths of Arctic pack ice, J. Acoust. Soc. Amer. 36, 1551-56, 1964.

6. Brown, J. R. and A. R. Milne, Reverberation under Arctic sea ice, J. Acoust. Soc. Amer. 42, 78-82, 1967.

7. Breslau, L. R., J. E. James, and M. D. Trammell, The underwater shape of a grounded ice island off Prudhoe Bay, Alaska, Paper OTC 1305, Offshore Technology Conference, Dallas, Texas, 1970.

8. Greischar, L. L. and C. S. Clay, Use of side-scanning sonar for contouring bottom features, J. Acoust. Soc. Amer. 51, 1073-75, 1972.

9. Chapman, R. P. and H. D. Scott, Backscattering strength of young sea ice, J. Acoust. Soc. Amer. 36, 2417-18, 1964.

10. Brown, J. R., Reverberation under Arctic ice, J. Acoust. Soc. Amer. 36, 601-3, 1964.

11. Mellen, R. H. and H. W. Marsh, Underwater sound reverberation in the Arctic Ocean, J. Acoust. Soc. Amer. 35, 1645-48, 1963.

12. Mellen, R. H., Underwater acoustic scattering from Arctic ice, J. Acoust. Soc. Amer. 40, 1200-2, 1966.

13. Greene, C. R., Underice acoustics at high frequencies, Technical Report TR 65-76, GM Defense Research Laboratories, Santa Barbara, California, 1965.

14. Brown, J. R. and D. W. Brown, Reverberation under Arctic sea ice, J. Acoust. Soc. Amer. 40, 399-404, 1966.

15. Langleben, M. P. and E. R. Pounder, Reflection of sound at the water-ice interface, Report S-16, Part II, MacDonald Physics Laboratory, McGill University, 20-30, 1970.